Bol. Soc. Paran. Mat.
©SPM – E-ISSN-2175-1188
SPM: www.spm.uem.br/bspm

(3s.) **v. 2026 (44) 4** : 1–16.
ISSN-0037-8712
doi:10.5269/bspm.80001

Gourava 2-Distance Degree Indices and QSPR Analysis of Alkanes

Sunita Priya D'Silva, Kunjaru Mitra, Chandrakala S. B.*, Sooryanarayana B. and Vishukumar M.

ABSTRACT: In mathematical chemistry, molecules are often represented as graphs and from these graphs, Topological indices(TIs) are derived, which are numerical values encoding structural information. TIs are introduced by Gutman and Trinajstić based on the degrees of the vertices and on distance between the vertices. QSPR analysis establishes correlations between TIs and measurable physicochemical properties. In this paper, few generalized topological indices are defined using the 2-distance degree of the vertices. This extension seeks to offer a more thorough understanding of network structures by capturing deeper connectivity patterns. The findings contribute to a better understanding of structure-property relationships in alkanes and can serve as a tool for predicting the properties of other alkanes based on their molecular structures.

Key Words: Distance in graph, molecular graph, topological indices.

Contents

1. Introduction

Understanding the relationship between molecular structure and physicochemical behavior remains a central theme in theoretical and computational chemistry. By translating molecular architecture into mathematical form, graph-theoretical approaches allow chemists to quantify how atomic connectivity governs macroscopic properties. In this framework, molecules are represented as graphs—atoms as vertices and bonds as edges—enabling structural analysis through numerical descriptors derived from connectivity patterns [6]. These descriptors, widely employed in quantitative structure–property relationship (QSPR) and quantitative structure–activity relationship (QSAR) studies, have proven particularly effective in modeling the behavior of hydrocarbons such as alkanes. Recent developments in distance-2 degree-based indices have further enhanced this predictive capability by capturing secondary atomic interactions that strongly influence key properties like boiling point, molar volume, and heat of vaporization refer [1], [16].

The degree of a vertex $v \in V$ of a connected graph $G(V, E)$ is the number of vertices which are at distance one from the vertex v and is denoted by $d(v)$. In this paper, 2-Distance degree-based topological indices were introduced to extend the classical degree-based descriptors by incorporating second-neighbor (distance two) interactions in molecular graphs. The concept of degree of a vertex is generalized as $i-$distance degree of a vertex $v \in V$ in a graph $G(V, E)$ with diameter, $diam(G) \geq i$, is defined as the number of vertices at the distance i from the vertex v is denoted by $d_i(v)$. If $d_2(v) = k, \forall v \in V(G)$, then G is called $2-$distance degree k regular graph. We introduce few topological indices based on $d_i(v)$ called $i-$distance degree topological indices in Table 1. In particular, study on $2-$distance degree topological indices are done. Through out the paper, let $E_{r,s} = \{uv : d_2(u) = r \text{ and } d_2(v) = s\}$.

Unlike traditional indices that consider only adjacent atoms, these indices capture the effect of atoms separated by two bonds, thereby providing a more nuanced picture of the molecule's topology. This approach has proven particularly effective for alkanes—acyclic hydrocarbons characterized by simple

* Corresponding author.
2020 *Mathematics Subject Classification:* 05C09, 05C92.
Submitted November 00, 2025. Published February 03, 2026

connectivity but variable branching—where subtle structural differences significantly influence physical and chemical properties. The First and Second Gourava Indices, proposed as 2− distance extensions of degree-based indices, measure molecular compactness and branching at the second level of atomic interaction [10], [15]. The First Gourava Index (GO_1^2) combines degree information of atoms and their second-neighbour connectivity, capturing how atomic environments influence molecular properties such as stability and boiling point. The Second Gourava Index (GO_2^2), on the other hand, incorporates a multiplicative relationship between the degrees of atoms at distance two, thereby emphasizing the cumulative branching effect across the molecular framework. These indices have demonstrated strong predictive capability for structural parameters and physicochemical properties of alkanes [11]. The Hyper Gourava Indices are nonlinear extensions of the Gourava indices, designed to magnify variations in atomic environments and capture higher-order connectivity effects.

The First Hyper Gourava Index (HGO_1^2) enhances the sensitivity of GO_1^2 by incorporating squared degree terms, which better reflect the influence of highly connected carbon atoms within the alkane structure. The Second Hyper Gourava Index (HGO_2^2) similarly extends GO_2^2 by amplifying the role of distant branching through a power-based relationship between vertex degrees. These hyper versions provide improved correlation with molecular descriptors and physicochemical properties such as molar refraction and heat of vaporization, as observed in recent QSPR studies [3], [4]. The Sum Connectivity Gourava Index (SCO^2), inspired by the general sum-connectivity index of Zhou and Trinajstić [18], considers the sum of vertex degrees at distance two instead of their product or square. This additive nature makes it particularly effective in distinguishing alkanes with similar degrees of branching but different chain lengths. It provides a balanced representation of molecular compactness and is often used alongside other Gourava indices to build robust QSPR models [14].

Alkanes, as saturated hydrocarbons, serve as fundamental model systems in molecular topology due to their simple yet structurally diverse frameworks. Their properties—boiling point (BP), melting point (MP), molar refraction (MR), heat of vaporization (HV), critical temperature (CT), and surface tension (ST)—are highly dependent on molecular size, shape, and branching [2,7,9]. Boiling Point (BP) reflects the strength of intermolecular forces, which increase with molecular size and branching complexity; topological indices can effectively quantify these variations. Melting Point (MP) depends on molecular symmetry and packing efficiency—parameters well captured by degree-based descriptors. Molar Refraction (MR) is linked to polarizability and molecular volume, making it highly responsive to topological features. Heat of Vaporization (HV) and Critical Temperature (CT) correlate with cohesive energy and molecular interactions, both of which are influenced by branching captured through distance-2 indices. Surface Tension (ST) reflects the intermolecular cohesion at phase boundaries, which can also be inferred from molecular connectivity patterns. Thus, distance-2 Gourava indices provide a mathematically grounded approach to understanding and predicting these properties, bridging molecular structure and macroscopic behavior [12,17]. Studies such as those by Chandrakala et al. [1] and Raja and Anuradha [11] have confirmed that these indices establish strong, often quadratic or linear, relationships with the physicochemical parameters of alkanes, validating their use in QSPR modeling. Hence, the 2− distance degree-based Gourava indices and their variants, including GO_1^2, GO_2^2, HGO_1^2, HGO_2^2, and SCO^2 are extend traditional topological descriptors by considering interactions beyond immediate atomic neighbors. Their ability to capture the subtle effects of molecular branching and connectivity makes them powerful tools for modeling and predicting the physical properties of alkanes. Through these indices, complex relationships between molecular topology and properties such as boiling point, molar refraction, and heat of vaporization can be quantitatively elucidated, advancing the predictive scope of chemical graph theory in hydrocarbon chemistry. For further studies of numerous kinds of topological indices of graphs and chemical structures, refer [2], [5], [7], [8], [10].

2. Basic Results

This section presents the computation of the newly introduced Gourava topological indices for different graph configurations, as summarized in Table 1. By analyzing 2-distance degree-based topological indices for standard graphs, reference values linked to specific molecular structures are obtained, which assist in predicting and characterizing chemical properties. The study not only highlights the mathematical characteristics of these indices, such as their structural sensitivity, computational behavior, and

Table 1: Definitions of i–distance degree Gourava Indices

Name of the indices	**Notation and Definition**
i–distance degree First Gourava Index	$GO_1^i(G) = \sum_{uv\in E}[d_i(u) + d_i(v) + d_i(u)d_i(v)]$
i–distance degree Second Gourava Index	$GO_2^i(G) = \sum_{uv\in E}[d_i(u)d_i(v)][d_i(u) + d_i(v)]$
i–distance degree First Hyper Gourava Index	$HGO_1^i(G) = \sum_{uv\in E}[d_i(u) + d_i(v) + d_i(u)d_i(v)]^2$
i–distance degree Second Hyper Gourava Index	$HGO_2^i(G) = \sum_{uv\in E}[(d_i(u)d_i(v))(d_i(u) + d_i(v))]^2$
i–distance degree Sum Connectivity Gourava Index	$SGO^i(G) = \sum_{uv\in E} \frac{1}{\sqrt{d_i(u)+d_i(v)+d_i(u)d_i(v)}}$

correlation with molecular parameters, but also underscores their potential use in molecular modeling and quantitative structure–property relationship (QSPR) analysis. Specifically, these indices can serve as valuable molecular descriptors that capture subtle variations in molecular topology, enabling researchers to establish predictive models that relate molecular structure to physicochemical properties, biological activities, and material performance.

Proposition 2.1 *In a graph G of order n, if $deg(v) = n - 1$, then $d_2(v) = 0$.*

Proposition 2.2 *In a graph G of order n if $deg(v) = 1$, then $1 \leq d_2(v) \leq n - 2$.*

Proposition 2.3 *For a $k-$regular connected graph G with order n and $1 < k < n - 1$, then $1 \leq d_2(v) \leq k(k - 1)$.*

Proposition 2.4 *For a graph G with order n, $d_2(v) \leq n - 1 - \delta$.*

Proof: For any vertex $v \in G$, $d(v) \geq \delta$ and $d_2(G) \leq n-1-d(v)$. Combining both we have the result. □

Theorem 2.5 *For a path $P_n(n \geq 3)$;*

(i) $GO_1^2(P_n) = \begin{cases} 7n - 19, & \text{for } 3 \leq n \leq 5 \\ 8(n - 3), & \text{for } n \geq 6 \end{cases}$

(ii) $GO_2^2(P_n) = \begin{cases} 0, & \text{for } n = 3 \\ 6, & \text{for } n = 4 \\ 16(n - 4), & \text{for } n \geq 5 \end{cases}$

(iii) $HGO_1^2(P_n) = \begin{cases} 2, & \text{for } n = 3 \\ 27, & \text{for } n = 4 \\ 68, & \text{for } n = 5 \\ 4(16n - 63), & \text{for } n \geq 6 \end{cases}$

(iv) $HGO_2^2(P_n) = \begin{cases} 0, & \text{for } n = 3 \\ 12, & \text{for } n = 4 \\ 80, & \text{for } n = 5 \\ 256n - 1200, & \text{for } n \geq 6 \end{cases}$

(v) $SGO^2(P_n) = \begin{cases} 2, & for\ n = 3 \\ 3\sqrt{3}, & for\ n = 4 \\ 2(\sqrt{3}+\sqrt{5}), & for\ n = 5 \\ 7.9362 + 2(n-5)\sqrt{2}, & for\ n \geq 6 \end{cases}$

Proof: Consider a path $P_n : v_1 - v_2 - ... - v_n$ on n vertices, in which 2−distance degree of vertices is given by $d_2(v_i) = \begin{cases} 1, & \text{for } i \in \{1, 2, n-1, n\} \\ 2, & \text{for } 3 \leq i \leq n-2 \end{cases}$ The edge set for $n = 3$ is $E_{1,0}$, for $n = 4$ is $E_{1,1}$, for $n = 5$ is $E_{1,1} \cup E_{2,1}$ and for $n \geq 6$ is $E_{1,1} \cup E_{1,2} \cup E_{2,2}$. Hence

(i) $GO_1^2(P_n) = \sum_{uv \in E} [d_2(u) + d_2(v) + d_2(u)d_2(v)]$
For $n = 3$, the $GO_1^2(P_n) = |E_{1,0}|[0 + 1 + 0] = 2 \cdot 1 = 7(3) - 19 = 2$
For $n = 4$, the $GO_1^2(P_n) = |E_{1,1}|[1 + 1 + 1] = 3 \cdot 3 = 7(4) - 19 = 9$
For $n = 5$, the $GO_1^2(P_n) = |E_{1,1}|[1 + 1 + 1] + |E_{2,1}|[1 + 2 + 2] = 7(5) - 19 = 16$
For $n \geq 6$, $GO_1^2(P_n) = |E_{1,1}|(1+1+1)+|E_{1,2}|(1+2+2)+|E_{2,2}|(2+2+4) = 2(3)+2(5)+(n-5)(8) = 8(n-3)$.

(ii) $GO_2^2(P_n) = \sum_{uv \in E} [d_2(u) + d_2(v)][d_2(u)d_2(v)]$
For $n = 3$, the $GO_2^2(P_n) = |E_{1,0}|[0 + 1][0] = 0$
For $n = 4$, the $GO_2^2(P_n) = |E_{1,1}|[1 + 1][1] = 6$
For $n \geq 5$, the $GO_2^2(P_n) = |E_{1,1}|([1+1][1])+|E_{2,1}|([1+2][2])+|E_{2,2}|([2+2][2 \cdot 2]) = 2 \cdot 2+2 \cdot 6+(n-5) \cdot 16 = 16(n-4)$

(iii) $HGO_1^2(P_n) = \sum_{uv \in E} [d_2(u) + d_2(v) + d_2(u)d_2(v)]^2$
For $n = 3$, the $HGO_1^2(P_n) = |E_{1,0}|[0 + 1 + 0]^2 = 2 \cdot 1 = 2$
For $n = 4$, the $HGO_1^2(P_n) = |E_{1,1}|[1 + 1 + 1]^2 = 3 \cdot 9 = 27$
For $n = 5$, the $HGO_1^2(P_n) = |E_{1,1}|[1 + 1 + 1]^2 + |E_{2,1}|[1 + 2 + 2]^2 = 2 \cdot 9 + 2 \cdot 25 = 68$
For $n \geq 6$, the $HGO_1^2(P_n) == |E_{1,1}|(1 + 1 + 1)^2 + |E_{1,2}|(1 + 2 + 2)^2 + |E_{2,2}|(2 + 2 + 4)^2 = 2(9) + 2(25) + (n-5)(64) = 4(16n - 63)$.
(iv) $HGO_2^2(P_n) = \sum_{uv \in E} ([d_2(u) + d_2(v)][d_2(u)d_2(v)])^2$
For $n = 3$, the $HGO_2^2(P_n) = |E_{1,0}|([0 + 1][0])^2 = 0$
For $n = 4$, the $HGO_2^2(P_n) = |E_{1,1}|([1 + 1][1])^2 = 2(4) = 8$
For $n = 5$, the $HGO_2^2(P_n) = |E_{1,1}|([1 + 1][1])^2 + |E_{2,1}|([1 + 2][2])^2 = 2 \cdot 4 + 2 \cdot 36 = 80$
For $n \geq 6$, the $HGO_2^2(P_n) = |E_{1,1}|([1 + 1][1])^2 + |E_{2,1}|([1 + 2][2])^2 + |E_{2,2}|([2 + 2][2 \cdot 2])^2 = 2 \cdot 4 + 2 \cdot 36 + (n-5) \cdot 64 = 256n - 1200$

(v) $SGO^2(P_n) = \sum_{uv \in E} [d_2(u) + d_2(v) + d_2(u)d_2(v)]^{-\frac{1}{2}}$
For $n = 3$, the $HGO_1^2(P_n) = |E_{1,0}|[0 + 1 + 0]^{-\frac{1}{2}} = 2 \cdot 1 = 2$
For $n = 4$, the $HGO_1^2(P_n) = |E_{1,1}|[1 + 1 + 1]^{-\frac{1}{2}} = 3 \cdot \sqrt{3} = 3\sqrt{3}$
For $n = 5$, the $HGO_1^2(P_n) = |E_{1,1}|[1 + 1 + 1]^{-\frac{1}{2}} + |E_{2,1}|[1 + 2 + 2]^{-\frac{1}{2}} = 2 \cdot 3\sqrt{3} + 2 \cdot \sqrt{5} = 2(\sqrt{3} + \sqrt{5})$
For $n \geq 6$, the $HGO_1^2(P_n) = |E_{1,1}|(1 + 1 + 1)^{-\frac{1}{2}} + |E_{1,2}|(1 + 2 + 2)^{-\frac{1}{2}} + |E_{2,2}|(2 + 2 + 4)^{-\frac{1}{2}} = 2(\sqrt{3}) + 2(\sqrt{5}) + (n-5)(\sqrt{8}) = 7.9362 + 2(n-5)\sqrt{2}$.

□

Theorem 2.6 *For a Cycle $C_n (n \geq 4)$;*

(i) $GO_1^2(C_n) = \begin{cases} 12, & for\ n = 4 \\ 8n, & for\ n \geq 5. \end{cases}$

(ii) $GO_2^2(C_n) = \begin{cases} 8, & for\ n = 4 \\ 16n, & for\ n \geq 5. \end{cases}$

(iii) $HGO_1^2(C_n) = \begin{cases} 36, & for\ n = 4 \\ 64n, & for\ n \geq 5. \end{cases}$

(iv) $HGO_2^2(C_n) = \begin{cases} 16, & \text{for } n = 4 \\ 256n, & \text{for } n \geq 5. \end{cases}$

(v) $SGO^2(C_n) = \begin{cases} \frac{4}{\sqrt{3}}, & \text{for } n = 4 \\ \frac{n}{2\sqrt{2}}, & \text{for } n \geq 5. \end{cases}$

Proof: For $n = 4$, $d_2(v) = 1$ and $n \geq 5$, $d_2(v) = 2, \forall v \in V(G)$. Also $E(C_4) = E_{1,1}$ and $E(C_n) = E_{2,2}$ for $n \geq 5$. Hence,

(i) For $n = 4$, $GO_1^2(C_n) = \sum_{uv \in E} [d_2(u) + d_2(v) + d_2(u)d_2(v)] = 4(1 + 1 + 1) = 12$.
For $n \geq 5$, $GO_1^2(C_n) = n(2 + 2 + 4) = 8n$.

(ii) For n=4, $GO_2^2(C_n) = \sum_{uv \in E} [d_2(u) + d_2(v)][d_2(u) \cdot d_2(v)] = 4(2 \cdot 1) = 8$.
For $n \geq 5$, $GO_2^2(C_n) = nE_{2,2} = n(2 + 2)(2 \cdot 2) = 16n$.

(iii) For $n = 4$, $HGO_1^2(C_n) = \sum_{uv \in E} [d_2(u) + d_2(v) + d_2(u)d_2(v)]^2 = 4E_{1,1} = 4(1 + 1 + 1)^2 = 36$.
For $n \geq 5$ $HGO_1^2(C_n) = nE_{2,2} = n(2 + 2 + 4)^2 = 64n$

(iv) For $n = 4$ $HGO_2^2(C_n) = \sum_{uv \in E} ([d_2(u) + d_2(v)][d_2(u) \cdot d_2(v)])^2 = 4(2 \cdot 1)^2 = 16$.
For $n \geq 5$, $HGO_2^2(C_n) = nE_{2,2} = n((2 + 2)(2 \cdot 2))^2 = 256n$.

(v) For $n = 4, SGO^2(C_n) = \sum_{uv \in E} [d_2(u) + d_2(v) + d_2(u) \cdot d_2(v)]^{-\frac{1}{2}} = 4(1 + 1 + 1) - \frac{1}{2} = \frac{4}{\sqrt{3}}$.
For $n \geq 5$, $SGO^2(C_n) = nE_{2,2} = n(2 + 2 + 4)^{-\frac{1}{2}} = \frac{n}{2\sqrt{2}}$.

□

Theorem 2.7 *For a Complete Bipartite graph $K_{p,q}, p > q \geq 2$;*

(i) $GO_1^2(K_{p,q}) = pq(pq - 1)$

(ii) $GO_2^2(K_{p,q}) = pq(p + q - 2)(p - 1)(q - 1)$

(iii) $HGO_1^2(K_{p,q}) = pq(pq - 1)^2$

(iv) $HGO_1^2(K_{p,q}) = pq((p - q - 2)(p - 1)(q - 1))^2$

(v) $SGO_1^2(K_{p,q}) = \frac{pq}{\sqrt{pq-1}}$

Proof: Let V_1 and V_2 be the partite vertex sets of $K_{p,q}$ then $d_2(v) = \begin{cases} p - 1, & \text{for } v \in V_1 \\ q - 1, & \text{for } v \in V_2. \end{cases}$ Then $E(K_{p,q}) = E_{p-1,q-1}$.

(i) $GO_1^2(K_{p,q}) = |E_{p-1,q-1}|(p - 1 + q - 1 + (p - 1)(q - 1)) = pq(pq - 1)$.

(ii) $GO_2^2(K_{p,q}) = |E_{p-1,q-1}|[(p - 1)(q - 1)][(p - 1)(q - 1)] = pq(p + q - 2)(p - 1)(q - 1)$.

(iii) $HGO_1^2(K_{p,q}) = |E_{p-1,q-1}|[(p - 1) + (q - 1) + (p - 1)(q - 1)]^2 = pq(pq - 1)^2$.

(iv) $HGO_2^2(K_{p,q}) = |E_{p-1,q-1}|[(p - 1)(q - 1)][(p - 1)(q - 1)]^2 = pq[(p + q - 2)(p - 1)(q - 1)]^2$.

(v) $SGO^2(K_{p,q}) = |E_{p-1,q-1}| \frac{1}{\sqrt{(p-1)+(q-1)+(p-1)(q-1)}} = \frac{pq}{\sqrt{pq-1}}$.

□

Theorem 2.8 *For a k-regular graph G of size m,*

(i) $GO_1^2(G) \leq mk(k - 1)(k^2 - k + 2)$.

(ii) $GO_2^2(G) \leq 2mk^3(k-1)^3$.

(iii) $HGO_1^2(G) \leq mk^2(k-1)^2(k^2-k+2)^2$.

(iv) $HGO_2^2(G) \leq 4mk^6(k-1)^6$

(v) $SGO^2(G) \leq \frac{m}{\sqrt{k(k-1)(k^2-k+2)}}$

Proof:

(i) $GO_1^2(G) = \sum_{uv\in E}[d_2(u)+d_2(v)+d_2(u)d_2(v)]$. From Proposition 2.3, $d_2(u) \leq k(k-1), \forall u \in V(G)$. Therefore, $GO_1^2(G) \leq \sum_{uv\in E}[k(k-1)+k(k-1)+k^2(k-1)^2] = \sum_{uv\in E} k(k-1)(k^2-k+2) = mk(k-1)(k^2-k+2)$.

(ii) $GO_2^2(G) = \sum_{uv\in E}[d_2(u)+d_2(v)][d_2(u)\cdot d_2(v)] \leq \sum_{uv\in E}[k(k-1)+k(k-1)][k(k-1)\cdot k(k-1)] = \sum_{uv\in E}[2k(k-1)][k^2(k-1)^2] = 2mk^3(k-1)^3$.

(iii) $HGO^2(G)_2 = \sum_{uv\in E}[d_2(u)+d_2(v)+d_2(u)d_2(v)]^2 \leq \sum_{uv\in E}[k(k-1)+k(k-1)+k^2(k-1)^2]^2 = \sum_{uv\in E} k^2(k-1)^2(k^2-k+2)^2 = mk^2(k-1)^2(k^2-k+2)^2$.

(iv) $HGO_2^2(G) = \sum_{uv\in E}([d_2(u)+d_2(v)][d_2(u)\cdot d_2(v)])^2 \leq \sum_{uv\in E}([k(k-1)+k(k-1)][k(k-1)\cdot k(k-1)])^2 = \sum_{uv\in E}[2k(k-1)]^2[k^2(k-1)^4] = 4mk^6(k-1)^6$

(v) $SGO^2(G) = \sum_{uv\in E}[d_2(u)+d_2(v)+d_2(u)d_2(v)]^{-\frac{1}{2}} \leq \sum_{uv\in E}\frac{1}{\sqrt{[k(k-1)+k(k-1)+k^2(k-1)^2]}} = \sum_{uv\in E}\frac{1}{\sqrt{k^2(k-1)^2(k^2-k+2)}} = \frac{m}{\sqrt{k(k-1)(k^2-k+2)}}$

□

Table 2: 2−**distance degree TIs of Alkanes**

No	Alkanes	GO_1^2	GO_2^2	HGO_1^2	HGO_2^2	SGO^2
1	2,2,3,3-Tetramethyl pentane	128	510	2168	37116	2.070224
2	2,2,3-Tetramethyl pentane	100	332	1358	17912	2.153531
3	2,2,4,4-Tetramethyl pentane	80	240	976	9648	2.153531
4	2,2,4-Tetramethyl pentane	68	156	632	4392	2.822487
5	2,2,4-Trimethyl hexane	72	176	710	6780	2.831261
6	2,2,4-Trimethyl hexane	53	108	439	3244	3.031261
7	2,2,5-Trimethyl hexane	59	122	499	3244	3.076129
8	2,2,-Di Methyl butane	20	60	245	720	1.889922
9	2,2-Dimethyl pentane	60	136	554	3672	2.116099
10	2,2-Dimethyl hexane	52	112	458	3176	2.37791
11	2,2-Dimethyl pentane	42	78	318	1236	2.759052
12	2,2-Dimethyl propane	6	0	28	0	3.309401
13	2,3-dimethyl-3-ethyl pentane	94	312	1280	17472	2.126668
14	2,3,3,4-Tetramethyl pentane	120	456	1928	31824	2.123708
15	2,3,3-Trimethyl hexane	109	358	1489	18908	2.81923
16	2,3,3-Trimethyl pentane	52	120	487	2532	2.852964
17	2,3,4-Trimethyl hexane	85	272	1133	13976	2.074068
18	2,3,4-Trimethyl pentane	74	208	844	7936	2.215997
19	2,3,5-Trimethyl hexane	76	208	862	9880	2.767396
20	2,3-Dimethyl butane	40	94	380	2280	1.767764
21	2,3-Dimethyl heptane	72	184	750	6168	2.894404
22	2,3-Dimethyl hexane	63	160	653	5376	2.523643
23	2,3-Dimethyl pentane	54	138	576	4248	2.059853
24	2,4-dimethyl-3-ethyl pentane	112	420	1784	30312	2.226815
25	2,4-Dimethyl heptane	62	140	570	4080	3.105401
26	2,4-Dimethyl hexane	54	118	480	3324	2.455521
27	2,4-Dimethyl pentane	38	66	262	944	2.385055
28	2,5-dimethyl-3-ethyl pentane	88	280	1148	15720	2.522249
29	2,5-Dimethyl heptane	74	184	748	5776	2.649342
30	2,5-Dimethyl hexane	49	102	423	3348	2.809082
31	2,6-Dimethyl heptane	56	108	440	2520	2.717808
32	2-Methyl heptane	46	68	278	728	1.788854
33	2-Methyl heptane	44	78	318	1412	2.295202

Table 2 – continued from previous page

No.	Alkanes	GO_1^2	GO_2^2	HGO_1^2	HGO_2^2	SGO^2
34	2-Methyl hexane	36	52	224	1156	2.596467
35	2-Methyl hexane	22	94	382	1668	2.566308
36	2-Methyl pentane	27	38	157	364	2.227706
37	3,3,4-Trimethyl hexane	81	224	911	8504	2.63558
38	3,3-Dimethyl butane	104	308	1264	15504	2.263521
39	3,3-Dimethyl heptane	70	178	724	4204	2.949666
40	3,3-Dimethyl hexane	60	144	584	4264	2.564527
41	3,4-Dimethyl heptane	52	116	468	2600	2.062409
42	3,4-Dimethyl hexane	78	218	898	8716	2.34240
43	3,4-Dimethyl hexane	69	186	759	6588	2.358671
44	3,5-Dimethyl heptane	70	172	698	5704	2.843163
45	3-Ethyl heptane	66	164	672	5728	2.081724
46	3-Ethyl hexane	57	140	575	4960	2.710862
47	3-Ethyl pentane	48	108	438	2808	2.246175
48	3-Ethyl-2-methyl hexane	78	232	964	12360	2.873573
49	3-Ethyl-2-methyl pentane	68	180	740	7440	2.404318
50	3-Ethyl-3-methyl pentane	90	292	1224	16496	2.070622
51	3-Ethyl-3-methyl pentane	81	252	1047	12096	2.166689
52	3-Methyl heptane	54	106	429	2388	2.818207
53	3-Methyl heptane	50	104	422	2352	2.867208
54	3-Methyl hexane	42	82	332	1596	2.414146
55	3-Methyl octane	59	122	493	2644	3.13546
56	3-Methyl pentane	40	80	322	960	1.952087
57	4,4-Dimethyl heptane	80	236	964	10024	2.906412
58	4-Ethyl heptane	64	166	688	6956	3.245001
59	4-Ethyl-2-methyl hexane	64	150	616	5004	3.02804
60	4-Methyl octane	60	128	519	3112	3.237968
61	Heptane	32	48	196	592	2.26635
62	Hexane	24	32	132	336	2.402681
63	Nonane	48	80	324	1104	3.40497
64	Octane	40	64	260	848	3.09788
65	Pentane	16	16	68	80	2.049128

3. QSPR Analysis of Alkanes employing 2−distance degree TIs

The correlation between the newly introduced graph invariant and various physicochemical properties of alkanes is examined using their hydrogen-depleted graph models. This analysis demonstrates how the invariant effectively captures structural variations that influence molecular behavior. Moreover, improved correlations are obtained by applying an optimally chosen weight function, defined below, which enhances the predictive capability of the invariant in modeling structure–property relationships.

Weight function: A weight function $\mathcal{W}$ is a mapping that assigns a real number to a given topological index. It is expressed as $\mathcal{W}(\mathcal{I}, \gamma) = \mathcal{I}^{\gamma}$, where γ is a real parameter representing the weight associated with the index $\mathcal{I}$.

The linear regression relationship used in this study is expressed as $y = m \log_2 (n \cdot x^{\gamma_o}) + b$ where (y) represents a given physical property of alkanes C_nH_{2n+2} and x denotes the corresponding topological index. The computed regression models for various properties are summarized in Table 3 to Table 6. In this expression, γ_o refers to the critical weight parameter where the value of γ that minimizes the least-squares error of the regression fit. Mathematically, this condition can be written as $\rho(y, ln(n \cdot x^{\gamma})) \leq \rho(y, ln(n \cdot x^{\gamma_o}))$ for every real γ.

Using this formulation, linear regression models have been developed for a range of physicochemical properties of alkanes, including Boiling Point (BP), Molar Volume (MV) at 20^0C, Molar Refraction (MR) at 20^0C, Heat of Vaporization (HV) at 25^0C, Critical Temperature (CT), and Surface Tension (ST) at 20^0C . These relationships are established using standard property data of the selected alkanes [1] in combination with the newly proposed topological indices.

In Table 3, all the examined properties exhibit strong positive correlations with GO_1^2, where Molar Refraction (MR) shows the highest correlation value (0.995681686) and Surface Tension (ST) the lowest (0.889337752). The Mean Square Error (MSE) analysis indicates that the model predicts MR and Heat of Vaporization (HV) with minimal error, reflecting their strong linear relationships with the topological index. However, the model performs less effectively for Boiling Point (BP) and Critical Temperature (CT), which show relatively higher error values. Although ST yields a low MSE, its weak correlation

Table 3: **QSPR analysis of alkanes (GO_1^2) with squared error sum**

Property	$P = m(\log_2(GO_1^2)^c) - b$	**Correlation**	**MSE**
BP	BP =137.4543815$(\log_2(GO_1^2)^{0.05})$ + 318.6688328	0.978572148	110035.1
MV	MV =72.18140062$(\log_2(GO_1^2)^{0.18})$ + 91.79512686	0.989706265	42030.62
MR	MR =24.20758883$(\log_2(GO_1^2)^{0})$ + 33.4188291	0.995681686	3518.537
HV	HV =20.71084$(\log_2(GO_1^2)^{0.23})$ + 37.0571	0.960869	3598.125
CT	CT =164.3409789$(\log_2(GO_1^2)^{-0.1})$ + 156.5662496	0.970602581	107805
ST	ST =8.62092452$(\log_2(GO_1^2)^{-0.12})$ + 2.044154065	0.889337752	50.79005

with the experimental data suggests that this parameter is not significantly influenced by the chosen topological index.

Table 4: **QSPR analysis of alkanes (GO_2^2) with squared error sum**

Property	$P = m(\log_2(GO_2^2)^c) - b$	**Correlation**	**MSE**
BP	BP =142.0032779$(\log_2(GO_2^2)^{0})$ + 312.5209989	0.977997567	311269.8
MV	MV =95.45691$(\log_2(GO_2^2)^{-0.05})$ + 91.0271	0.989438	41727.45
MR	MR =24.20758883$(\log_2(GO_2^2)^{0})$ + 33.4188291	0.995681686	3518.537
HV	HV =28.10176274$(\log_2(GO_2^2)^{-0.05})$ + 35.78664805	0.955172519	3467.562
CT	CT =155.58928$(\log_2(GO_2^2)^{0.003})$ + 213.4156567	0.975367269	146053.5
ST	ST =10.39405$(\log_2(GO_2^2)^{0.015})$ + 2.67438	0.887592	46.374533

In Table 4, Molar Refraction (MR) shows the strongest correlation (0.995681686) and the low MSE (3518.537), indicating that it provides the most reliable and accurate predictive model among all the examined properties. Although Surface Tension (ST) also exhibits a low MSE value (46.374533), its weak correlation (0.887592) suggests that the model has limited predictive capability for this property. Conversely, Boiling Point (BP) displays the highest MSE (311269.8), implying that despite its positive correlation, the large prediction error reduces the practical significance of this relationship, making the correlation less meaningful for BP prediction.

In Table 5, a strong linear correlation is observed between HGO_1^2 and the parameter MV, as indicated by their nearly perfect positive correlation coefficient of 0.9957. Similarly, the correlation between HGO_1^2 and MR is also strong, with a coefficient of 0.9905, which, although slightly lower than that of MV,

Table 5: **QSPR analysis of alkanes (HGO_1^2) with squared error sum**

Property	$P = m(\log_2(HGO_1^2)^c) - b$	**Correlation**	**MSE**
BP	$BP = 131.7040043(\log_2(HGO_1^2)^{-0.03}) + 311.9364359$	0.9776835	105736.1
MV	$MV = 92.47061908(\log_2(HGO_1^2)^{-0.04}) + 82.14515078$	0.990472283	38162.23
MR	$MR = 24.20758883(\log_2(HGO_1^2)^{0}) + 33.4188291$	0.995681686	3518.537
HV	$HV = 26.33769918(\log_2(HGO_1^2)^{-0.03}) + 33.23910945$	0.956476667	3176.789
CT	$CT = 151.0680904(\log_2(HGO_1^2)^{0.05}) + 232.5612381$	0.973053546	161249.5
ST	$ST = 5.947435181(\log_2(HGO_1^2)^{0.1}) + 2.372559331$	0.899717835	46.3373

still signifies a highly linear relationship. However, when considering the mean square error (MSE), MR shows a smaller MSE value compared to MV, suggesting that the predictive model for MR provides more accurate estimations. Furthermore, the MSE values for HV are relatively low, yet the corresponding correlation is weaker than that of MR, indicating a moderate but consistent relationship. For BP, HV, CT, and ST, the correlation coefficients of 0.97, 0.95, and 0.899 suggest more complex, less direct relationships between these properties and the HGO_1^2 index. Additionally, the higher MSE values for BP, CT, and ST imply reduced model accuracy, indicating that these properties are influenced by more intricate or non-linear interactions with the topological index.

Table 6: **QSPR analysis of alkanes (HGO_2^2) with squared error sum**

Property	$P = m(\log_2(HGO_2^2)^c) - b$	**Correlation**	**MSE**
BP	$BP = 141.2063975(\log_2(HGO_2^2)^{0}) + 310.075423$	0.977540907	307449.5
MV	$MV = 85.87408(\log_2(HGO_2^2)^{-0.01}) + 85.8586$	0.988438	39689.75
MR	$MR = 24.20758883(\log_2(HGO_2^2)^{0}) + 33.4188291$	0.995681686	3518.537
HV	$HV = 23.68685068(\log_2(HGO_2^2)^{0}) + 32.48284566$	0.950902688	3111.016
CT	$CT = 158.2900627(\log_2(HGO_2^2)^{0.012}) + 207.7734789$	0.975257151	141889
ST	$ST = 6.426202(\log_2(HGO_2^2)^{0.04}) + 1.44233$	0.90037	46.052583

Table 6 demonstrates that HGO_2^2 exhibits strong linear correlations with the properties MV and MR, with correlation coefficients exceeding 0.98. This indicates a strong predictive relationship between these parameters. Moreover, the relatively low MSE value for MR suggests that the corresponding model can predict MR with good accuracy. In contrast, although MV also shows a high correlation, its larger MSE

value implies greater prediction error and reduced reliability.

For ST, the correlation coefficient is around 0.90, representing a comparatively weaker or more complex relationship with HGO_2^2. Despite its low MSE, the reduced correlation indicates that the model does not capture the underlying dependency effectively, reflecting limited accuracy in predicting this property.

Table 7: **QSPR analysis of alkanes (SGO^2) with squared error sum**

Property	$P = m(\log_2(SGO^2)^c) - b$	**Correlation**	**MSE**
BP	BP =140.7894025$(\log_2(SGO^2)^{0.01})$ + 311.0997887	0.977766531	105206.6
MV	MV =75.55119067$(\log_2(SGO^2)^{0.1})$ + 75.31186978	0.988315953	35630.15
MR	MR =24.20758883$(\log_2(SGO^2)^{0})$ + 33.4188291	0.995681686	3518.537
HV	HV =21.30452315$(\log_2(SGO^2)^{0.17})$ + 30.24176105	0.957702722	2852.226
CT	CT =164.4248953$(\log_2(SGO^2)^{-0.05})$ + 192.2990162	0.973329592	131150.9
ST	ST =8.838714104$(\log_2(SGO^2)^{-0.15})$ + 3.833936205	0.892855722	49.32061

According to Table 7, a strong linear correlation is observed between SCO^2 and the molecular property MR, similar to other topological indices, with a correlation coefficient of 0.9957, indicating an almost perfect positive relationship. Although the property HV exhibits a relatively low MSE value, it is not considered to be strongly correlated due to its lower correlation coefficient compared to MR. The MR parameter, on the other hand, demonstrates both a very high correlation and a low MSE, confirming it as the most reliable predictor among the studied properties.

Except for ST, which shows a comparatively weaker correlation despite having a lower MSE, all other properties exhibit strong positive correlations with SCO^2, though their higher MSE values suggest greater prediction variability. Overall, these findings emphasize that SCO^2 serves as a robust topological descriptor for predicting MR, while its relationship with other molecular properties is characterized by varying degrees of correlation strength and predictive accuracy.

Table 8: **Summary of Critical Points (c) and Correlation coefficients (r) for Different Gourava Topological Indices**

	GO_1^2		GO_2^2		HGO_1^2		HGO_2^2		SGO^2	
Property	c	r	c	r	c	r	c	r	c	r
BP	0.05	0.9786	0.000	0.9780	0.03	0.9777	0.000	0.9775	0.01	0.9778
MV	0.18	0.9897	-0.050	0.9894	-0.04	0.9905	-0.010	0.9884	0.10	0.9883
MR	0.00	**0.9957**	0.000	**0.9957**	0.00	**0.9957**	0.000	**0.9957**	0.00	**0.9957**
HV	0.23	0.9609	-0.050	0.9552	-0.03	0.9565	0.000	0.9509	0.17	0.9577
CT	-0.10	0.9706	0.008	0.9754	0.05	0.9731	0.012	0.9753	-0.05	0.9733
ST	-0.12	0.8893	0.080	0.8876	0.10	0.8997	0.040	0.9004	-0.15	0.8929

Table 8 presents the summary of critical values along with the correlation coefficients between the Gourava topological indices and various physicochemical properties. The critical value represents the statistical threshold used to test the null hypothesis—that there is no significant difference between the experimentally determined (standard) values of the properties of the alkanes and the values predicted using the topological indices.

For the molecular volume (MV), the critical values are found to be zero, indicating that the observed and predicted values are statistically indistinguishable. Moreover, MV exhibits a high correlation with all the Gourava topological indices, suggesting a strong and consistent linear relationship. This implies that the null hypothesis can be accepted across all indices, confirming that the Gourava topological indices are highly reliable predictors of the molecular volume property of alkanes.

4. Analysis with Gamma(γ)-curve

The $\gamma(x, y)-$curve of property y with respect to the topological index x is a curve on $xy-$plane drawn $\rho(y, ln(n \cdot x^{\gamma}))$ versus γ. The $\gamma-$curves of physical properties of alkanes with respect to GO_1^2, GO_2^2, HGO_1^2, HGO_2^2 and SGO^2 are shown in Figure 1 to 5.

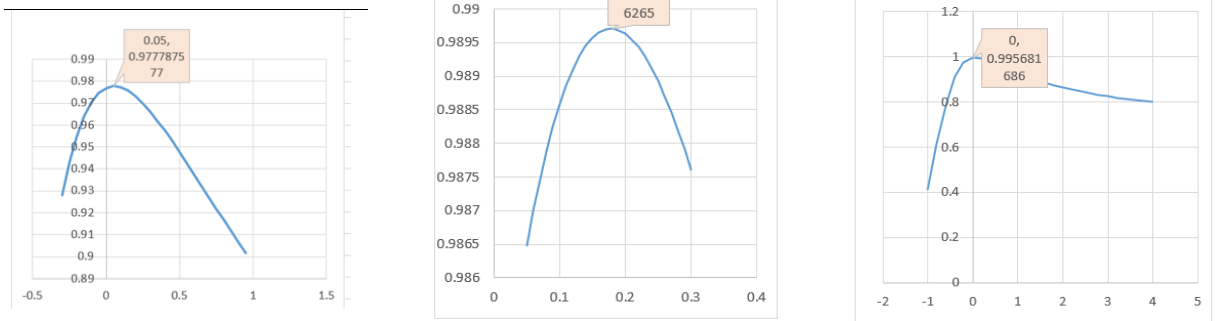

(a) $GO_1^2 - BP$ (b) $GO_1^2 - MV$ (c) $GO_1^2 - MR$

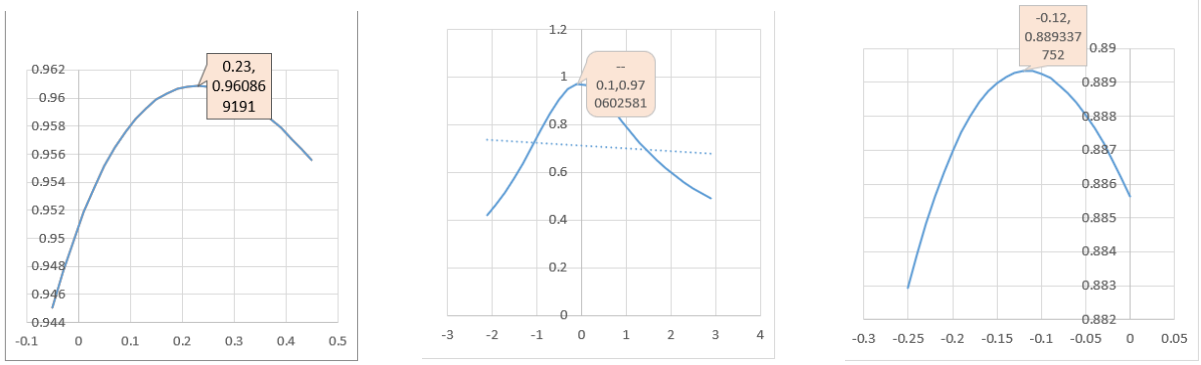

(d) $M_1^2 - HV$ (e) $M_1^2 - CT$ (f) $M_1^2 - ST$

Figure 1: Graph of correlation curves of GO_1^2 with various taken over critical point

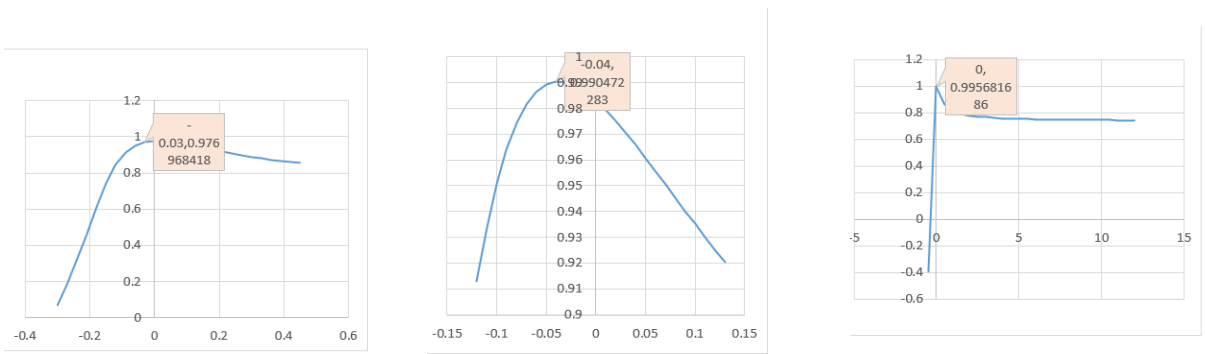

(a) $HGO_1^2 - BP$ (b) $HGO_1^2 - MV$ (c) $HGO_1^2 - MR$

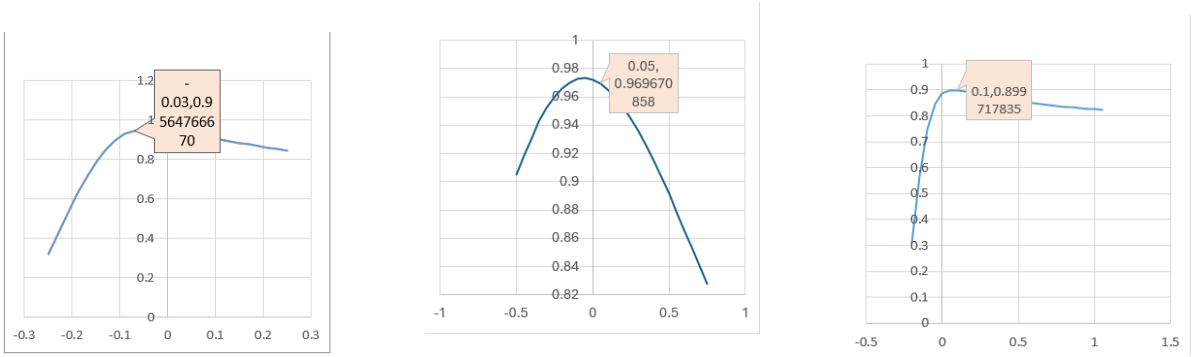

(d) $HGO_1^2 - HV$ (e) $HGO_1^2 - CT$ (f) $HGO_1^2 - ST$

Figure 3: Graph of correlation curves of HGO_1^2 with critical point

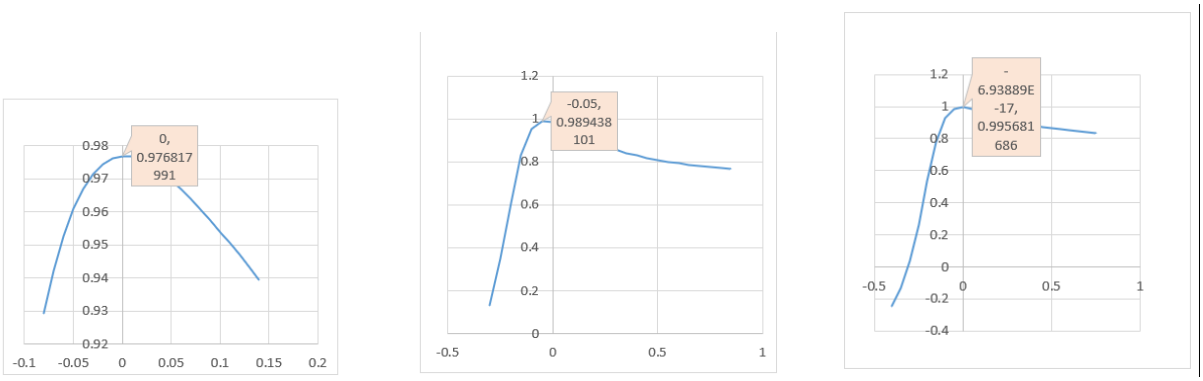

(a) $GO_2^2 - BP$ (b) $GO_2^2 - MV$ (c) $GO_2^2 - MR$

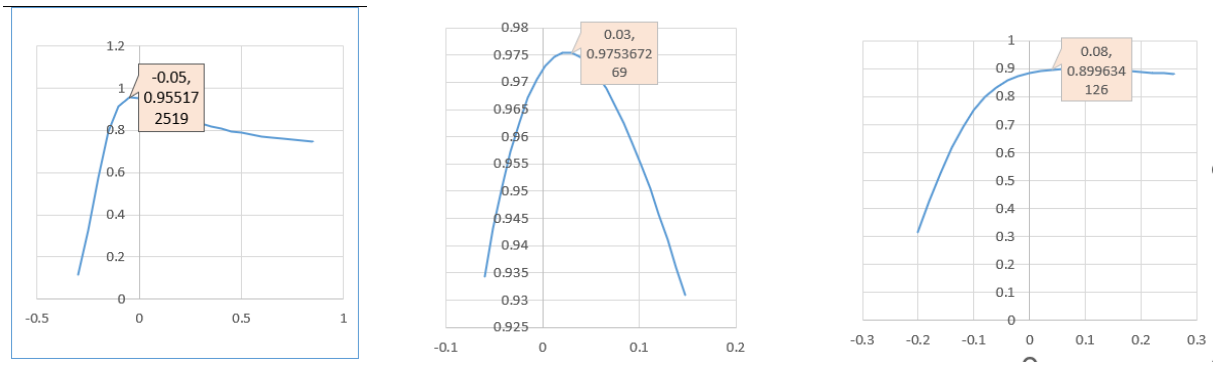

(d) $GO_2^2 - HV$ (e) $GO_2^2 - CT$ (f) $GO_2^2 - ST$

Figure 2: Graph of correlation curves of GO_2^2 with critical point

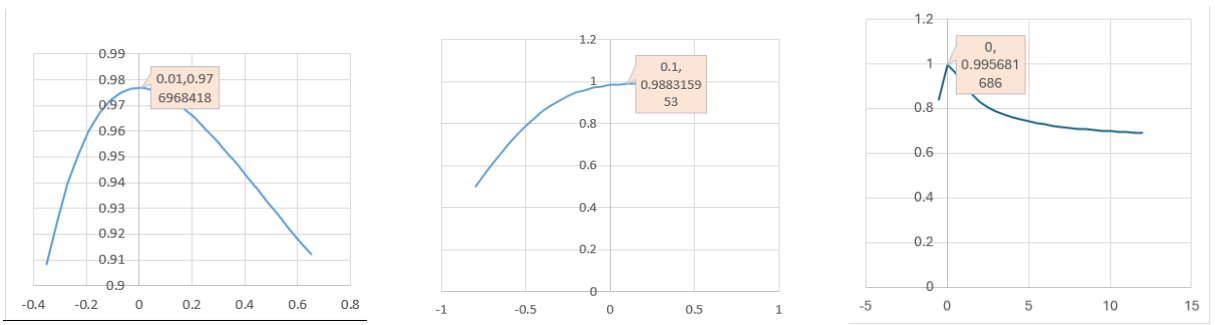

(a) $SGO^2 - BP$ (b) $SGO^2 - MV$ (c) $SGO^2 - MR$

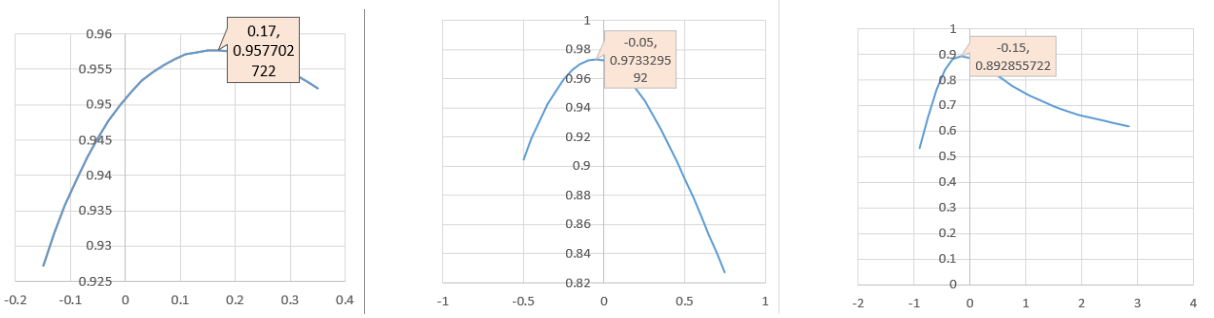

(d) $SGO^2 - HV$ (e) $SGO^2 - CT$ (f) $SGO^2 - ST$

Figure 5: Graph of correlation curves of SGO^2 with critical point

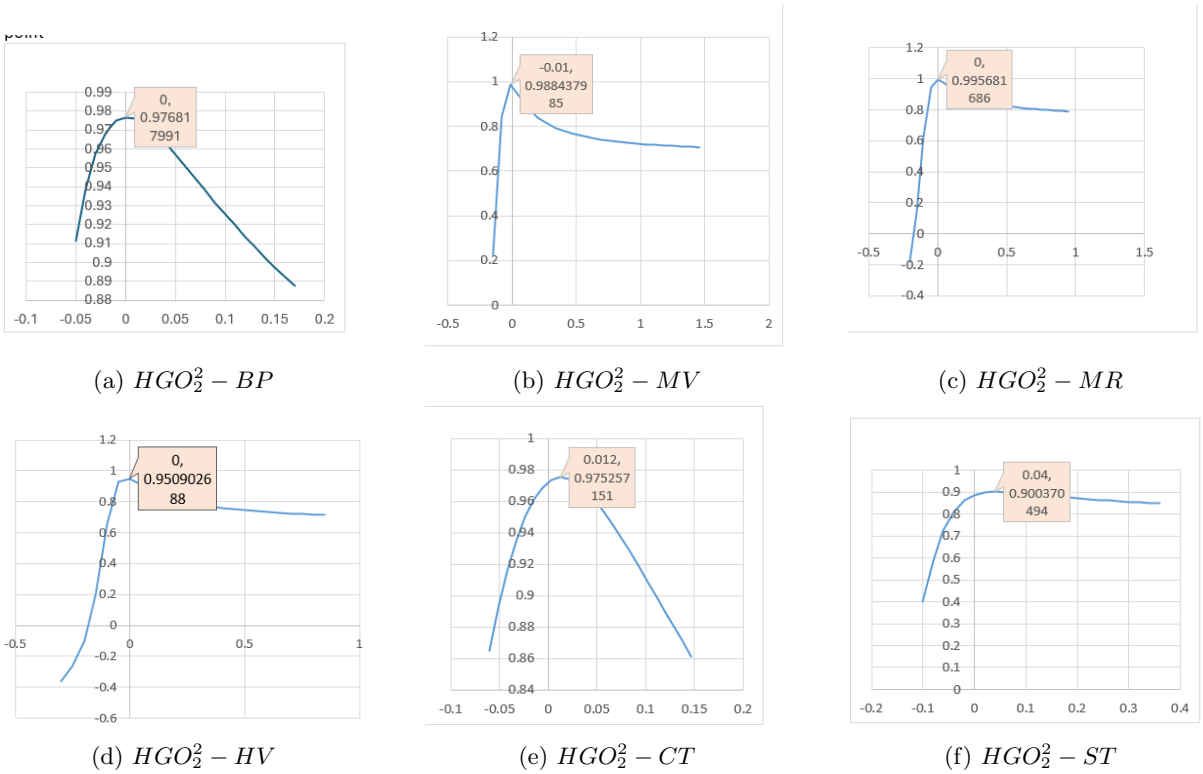

(a) $HGO_2^2 - BP$ (b) $HGO_2^2 - MV$ (c) $HGO_2^2 - MR$

(d) $HGO_2^2 - HV$ (e) $HGO_2^2 - CT$ (f) $HGO_2^2 - ST$

Figure 4: Graph of correlation curves of HGO^2 with critical point

The curves presented in Graph 1 reveal that even slight variations in Molar Refraction (MR) can significantly influence the correlation, as each property exhibits a distinct optimal value for the descriptor. This observation highlights specific regions where the model could be refined, particularly for parameters such as Heat of Vaporization, Boiling Point, and Critical Temperature. From Graphs 2c, 4c, 3c, and 5c, it is evident that the BP, MV, HV, CT and ST plots display a well-defined parabolic pattern. This characteristic shape suggests the presence of a quadratic relationship between the corresponding molecular property and the different Gourava topological indices. In other words, as the values of Gourava topological indices increase, the associated property first changes at an increasing or decreasing rate up to a certain point and then reverses direction, forming a curve that resembles a parabola. Such a trend highlights that the variation in property is not linear but instead depends on the square of index value, reflecting a more complex and non-linear correlation between the molecular structure and its physico-chemical or biological property.

5. Conclusion

The QSPR analysis provides valuable insights into the relationship between molecular structure and physicochemical properties of alkanes. The developed models effectively predict key properties—boiling point (BP), molar volume (MV), molar refractivity (MR), heat of vaporization (HV), critical temperature (CT), and surface tension (ST)—based on the chemical structure of the compounds.

The study reveals that these physical properties are significantly influenced by the distance-2 topological indices ($(GO_1^2, GO_2^2, HGO_1^2, HGO_2^2$, and $SGO^2)$. All Gourava indices exhibit strong positive correlations with the studied properties, confirming their structural sensitivity. Among them, MR stands out as the most reliable descriptor, showing both high correlation and low mean square error (MSE) with a zero critical value, thereby supporting the null hypothesis that no significant deviation exists between predicted and experimental values.

The analysis of molar refraction (MR) further highlights its importance in understanding molecular

size, shape, and polarizability. However, models for surface tension (ST) demonstrate relatively higher errors and weaker correlations, suggesting the need for incorporating additional molecular descriptors to enhance predictive accuracy. Overall, the findings establish Gourava topological indices as powerful tools for predicting and interpreting the structural-property relationships in alkanes.

References

1. Chandrakala, S. B., Sooryanarayana, B. and Roshini, G. R., *Analysis of Distance 2 Topological Models of Alkanes*, Biointerface Res. Appl. Chem. 13(4), 307, (2023).
2. Estrada, E., Torres, L., Rodrguez, L., and Gutman, I., *An atom-bond connectivity index: modeling the enthalpy of formation of alkanes*, Indian J. Chem. A, 37, 849–855, (1998).
3. Ediz, S., *On ve-degree molecular topological properties of silicate and oxgen networks*, Int. J. Comput. Sci. Math., 9(1), 1-12, (2018).
4. Farahani, M. R., *Connectivity indices of pent-heptagonal nanotubes $VAC_5C_7[p,q]$*, Adv. Mater. Corros., 2(1), 33–35, (2013).
5. Furtula, B., Graovac, A., and Vukičević, D., *Augmented Zagreb index*, J. Math. Chem., 48(2), 370–380, (2010).
6. Gutman, I., Trinajsti´c, N., *Graph theory and molecular orbitals. III. Total p-electron energy of alternate hydrocarbons*, Chem. Phys. Lett, 17, 535–538, (1972).
7. Sardar, M. S., Ali, M. A., Farahani, M. R., *Degree-Based Topological Indices Of Alkanes By Applying Some Graph Operations*, European Chemical Bulletin, 12(5), 39-50, (2023).
8. Gao, Y., Sajjad, W., Baig, A. Q., Farahani, M. R., *The Edge Version of Randic, Zagreb, Atom Bond Connectivity and Geometric-Arithmetic indices of $HAC_5C_6C_7$ nanotube*, Int. J. Pure Appl. Math., 115(2), 405-418, (2017).
9. Manso, F. C. G., Júnior, H. S., Bruns, R. E., Rubira, A. F., Muniz, E. C., *Development of a new topological index for the prediction of normal boiling point temperatures of hydrocarbons: The Fi index*, J. Mol. Liquids, 165, 125–132, (2012).
10. Poojary, P., Raghavendra, A., Shenoy, B. G., Farahani, M. R., and Sooryanarayana, B., *Certain topological indices and polynomials for the Isaac graphs*, J. Discret. Math. Sci. Cryptogr, 24(2), 511-525, (2021).
11. Raja, N.J.M.M., Anuradha, J., *A Bonding alkane attributes with topological indices: a statistical intervention*, J. Math. Chem., 62, 2889–2911, (2024).
12. Raza, I. Z. and Sukaiti, E. K., *M-polynomial and degree based topological indices of some nanostructures*, Symmetry, 12(5), 831, (2020).
13. Roshini, G. R. and Chandrakala, S. B., *Multiplicative Zagreb Indices of Transformation Graphs*, Anusandhana J. Sci. Eng. Manage., 6(1), 18-30, (2018).
14. Roshini, G. R., Chandrakala, S. B. and Sooryanarayana, B., *some degree based topological indices of transformation graphs*, Bull. Int. Math. Virtual Inst., 10(2), 225-237, (2020).
15. Sooryanarayana, B., Chandrakala, S. B. and Roshini, G. R., *On Realization and Characterization of Topological Indices*, Int. J. Innovat. Technol. Explor. Eng., 9(1), 715-718, (2019).
16. Sooryanarayana, B., Chandrakala, S. B., and Roshini, G. R., *Zagreb indices at a distance 2*, J. Math. Comput. Sci. C, 10(3), 639-655, (2020).
17. Zhang, X., Sajjad, W., Baig, A. Q., and Farahani, M. R., *The edge version of degree based topological indices of p NAqp nanotube*, Appl. Math., 08(10), 1445–1453, (2017).
18. Zhou, B. and Trinajstic, N., *On general sum-connectivity index*, J. Math. Chem., 47(1), 210–218, (2010).

Sunita Priya D'Silva.,
Department of Mathematics,
Sahyadri College of Engineering and Management, Mangaluru, India.
E-mail address: sunitapriya11@gmail.com

and

Kunjaru Mitra.,
Department of Mathematics,
Mangalore Institute of Technology & Engineering , Mangaluru, India
India.
E-mail address: mitrakunjaru@gmail.com

and

Chandrakala S.B.,
Department of Mathematics,
Nitte Meenakshi Institute of Technology, NITTE (Deemed to be University), Bengaluru, India
E-mail address: chandrakalasb14@gmail.com

and

Sooryanarayana B.,
Department of Mathematics
Nitte Meenakshi Institute of Technology, NITTE (Deemed to be University), Bengaluru, India
E-mail address: dr_bsnrao@yahoo.co.in

and

Vishukumar M.,
Department of Mathematics, School of Applied Sciences, Reva University,
India.
E-mail address: vishukumarm@reva.edu.in